

# A Soluble and Stable Quinoidal Bisanthene with NIR Absorption and Amphoteric Redox Behavior

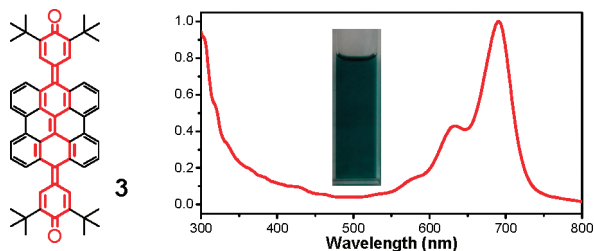
Kai Zhang, Kuo-Wei Huang, Jinling Li, Jing Luo, Chunyan Chi, and Jishan Wu\*

Department of Chemistry, National University of Singapore,  
3 Science Drive 3, Singapore, 117543

chmwuj@nus.edu.sg

Received August 18, 2009

## ABSTRACT



A soluble and stable quinoidal bisanthene (**3**) was synthesized, and it exhibited high molar absorptivity in the near-IR spectral region. In addition, compound **3** also showed good electrochemical amphotericity with four reversible one-electron transfer steps. Compound **3** represents a rare example of soluble and stable  $\pi$ -conjugated polycyclic hydrocarbons with quinoidal character.

Quinoidal structure plays an important role in determining the electronic and optical properties of  $\pi$ -conjugated systems.<sup>1</sup> For example, oxidative doping of conjugated polymers such as polypyrrole resulted in formation of radical cations (polarons) along the polymer chain with quinoidal character, which account for the long wavelength absorption in the doped state.<sup>2</sup> A neutral poly(isothianaphthene) as a prototype of small band gap polymers also contains a quinoidal structure in the main chain.<sup>3</sup> Several linear  $\pi$ -conjugated quinones or dicyanoquinodimethanes extended by phenyl<sup>4</sup> or five-membered heteroaromatics<sup>5</sup> (i.e., thienylene, furylene, etc.) have been reported and showed intense near-infrared (NIR) absorption. Moreover, a quinoidal porphyrin displays an absorption spectrum at the far-red spectral region, which is significantly different from normal aromatic porphyrins.<sup>6</sup> Usually, the quinoidal  $\pi$ -conjugated systems exhibit a lower

band gap in comparison with their aromatic analogues, and thus, materials with broad absorption in the visible-to-NIR spectral range are normally obtained. In addition, quinoidal compounds such as extended benzoquinones have frequently shown electrochemical amphoteric redox behavior; i.e., the materials can be easily oxidized and reduced by a multistage electron transfer with a small span of the oxidation and reduction potentials.<sup>4,5,7</sup> The multistage redox properties as well as the long-wavelength absorption make the quinoidal compounds useful for many applications such as NIR dyes

(5) (a) Takahashi, K.; Suzuki, T.; Akiyama, K.; Ikegami, Y.; Fukazawa, Y. *J. Am. Chem. Soc.* **1991**, *113*, 4576–4583. (b) Rao, V. P.; Jen, A. K.-Y.; Wong, K. Y.; Drost, K. J. *J. Chem. Soc., Chem. Commun.* **1993**, 1118–1120. (c) Kawai, S. H.; Gilat, S. L.; Lehn, J.-M. *J. Chem. Soc., Chem. Commun.* **1994**, 1011–1013. (d) Takahashi, K.; Tomitani, K. *J. Chem. Soc., Chem. Commun.* **1995**, 821–822. (e) Takahashi, K.; Gunji, A.; Yanagi, K.; Miki, M. *J. Org. Chem.* **1996**, *61*, 4784–4792. (f) Dimroth, K.; Umbach, W.; Blocher, K. H. *Angew. Chem., Int. Ed. Engl.* **1963**, *2*, 620–621. (g) Takahashi, T.; Matsuoka, K.; Takimiya, K.; Otsubo, T.; Aso, Y. *J. Am. Chem. Soc.* **2005**, *127*, 8928–8929.

(6) Blake, I. M.; Anderson, H. L.; Beljonne, D.; Brédas, J. L.; Clegg, W. *J. Am. Chem. Soc.* **1998**, *120*, 10764–10765.

(7) (a) Heimis, T.; Chowhury, S.; Scott, S. L.; Kebarle, P. *J. Am. Chem. Soc.* **1988**, *110*, 400–407. (b) Kurata, H.; Tanaka, T.; Oda, M. *Chem. Lett.* **1999**, 749–750.

(1) Brédas, J. L. *J. Chem. Phys.* **1985**, *82*, 3808–3811.

(2) Brédas, J. L.; Street, G. B. *Acc. Chem. Res.* **1985**, *18*, 309–315.

(3) Wudl, F.; Kobayashi, M.; Heeger, A. J. *J. Org. Chem.* **1984**, *49*, 3382–3384.

(4) West, R.; Jorgenson, J.; Stearley, K.; Calabrese, J. J. *J. Chem. Soc., Chem. Commun.* **1991**, 1234–1235.

and pigments,<sup>8</sup> electrical conductors,<sup>9</sup> ambipolar field effect transistors,<sup>10</sup> solar cells,<sup>11</sup> and nonlinear optics.<sup>12</sup>

To prepare materials with high electrochemical amphotericity and long wavelength absorption, one strategy is to construct large  $\pi$ -conjugated systems by (i) increasing the quinoidal character, (ii) increasing the rigidification of the  $\pi$ -system into a nearly planar conformation, and (iii) introducing electron-donating and electron-accepting moieties along the conjugated chain.<sup>13</sup> Polycyclic aromatic hydrocarbons (PAHs) with large  $\pi$ -conjugation and rigid planar structure have proven to be not only exciting objects for structural chemists but also important opto-electronic materials for material scientists due to their many potential applications for organic electronic devices.<sup>14</sup> Quinoidal PAHs are expected to be another type of interesting material with intriguing properties. However, to the best of our knowledge, there are few reports about design and synthesis of soluble and stable quinoidal PAHs with electrochemical amphotericity. Some quinones of active PAHs such as oligoacenes are known, but the quinones of larger  $\pi$ -conjugated PAHs are usually insoluble.<sup>15</sup>

Our recent goal is to prepare soluble and stable NIR dyes by using zigzag edged nanographenes such as periacenes as building block which are supposed to have small band gaps.<sup>16</sup> Among them, the bisanthene (**1**, Figure 1) represents an interesting object with absorption maximum at 662 nm.<sup>17</sup> However, bisanthene **1** is a very unstable compound due to its high-lying HOMO energy level, and thus, attachment of electron withdrawing groups such as carboximides is necessary to prepare stable bisanthene derivatives with NIR absorption.<sup>18</sup> On the other hand, the bisanthene quinone (**2**)

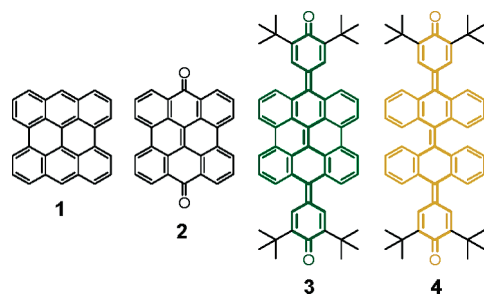


**Figure 1.** Molecular structures of bisanthene (**1**), bisanthene quinones (**2** and **3**), and bisanthracenequinone (**4**).

was found to be very stable, but it is virtually insoluble in most organic solvents and difficult to process. Thus, our objective is to prepare the di-*tert*-butyl-substituted extended bisanthenequinone **3** which is supposed to possess larger  $\pi$ -conjugation along the long axis and better solubility than the bisanthenequinone **2**. Consequently, intense NIR absorption and electrochemical amphotericity are expected from compound **3** due to its quinoidal character and large delocalized structure. For the sake of comparison, an extended bisanthracenequinone **4** with a twisted structure was also prepared.

The synthesis of quinones **3** and **4** is outlined in Scheme 1. The bisanthracenequinone **5** and bisanthenequinone **2** were

(8) Fabian, J.; Nakanzumi, H.; Matsuoka, M. *Chem. Rev.* **1992**, *92*, 1197–1226.

(9) (a) Ferraris, J. P.; Cowan, D. O.; Walatka, V.; Perlstein, J. P. *J. Am. Chem. Soc.* **1973**, *95*, 948–949. (b) Torrance, J. B.; Mayerle, J. J.; Lee, V. Y.; Bechgard, K. *J. Am. Chem. Soc.* **1979**, *101*, 4747–4748. (c) Dumur, F.; Gautier, N.; Gallego-Planas, N.; Sahin, Y.; Levillain, E.; Mercier, N.; Hudhomme, P.; Masino, M.; Girlando, A.; Lloveras, V.; Vidal-Gancedo, J.; Veciana, J.; Rovira, C. *J. Org. Chem.* **2004**, *69*, 2164–2177. (d) Matsumoto, T.; Sugimoto, T.; Noguchi, S. *Synth. Met.* **2003**, *135*, 571–572.

(10) (a) Pappenfus, T. M.; Chesterfield, R. J.; Frisbie, C. D.; Mann, K. R.; Casado, J.; Raff, J. D.; Miller, L. L. *J. Am. Chem. Soc.* **2002**, *124*, 4184–4185. (b) Pappenfus, T. M.; Raff, J. D.; Hukkanen, E. J.; Burney, J. R.; Casado, J.; Drew, S. M.; Miller, L. L.; Mann, K. R. *J. Org. Chem.* **2002**, *67*, 6015–6024. (c) Chesterfield, R. J.; Newman, C. R.; Pappenfus, T. M.; Ewbank, P. C.; Haukaas, M. H.; Mann, K. R.; Miller, L. L.; Frisbie, C. D. *Adv. Mater.* **2003**, *15*, 1278–1282.

(11) (a) Tamizhmani, G.; Dodelet, J. P.; Cote, R.; Gravel, D. *Chem. Mater.* **1991**, *3*, 1046–1053. (b) Yu, H. A.; Kaneko, Y.; Yoshimura, S.; Otani, S. *Appl. Phys. Lett.* **1996**, *68*, 547–549.

(12) Higuchi, H.; Nakayama, T.; Koyama, H.; Ojima, J.; Wada, T.; Sasabe, H. *Bull. Chem. Soc. Jpn.* **1995**, *68*, 2363–2377.

(13) Roncali, J. *Chem. Rev.* **1997**, *97*, 173–205, and references therein.

(14) (a) Watson, M. D.; Fechtenkötter, A.; Müllen, K. *Chem. Rev.* **2001**, *101*, 1267–1300. (b) Wu, J.; Pisula, W.; Müllen, K. *Chem. Rev.* **2007**, *107*, 718–747.

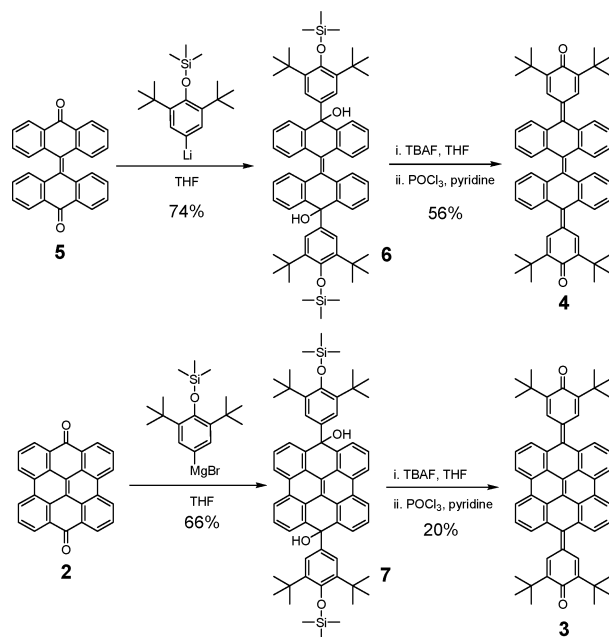
(15) (a) Clar, E. *Polycyclic Hydrocarbons*; Academic Press: London, 1964; Vol. 2. (b) Koch, W.; Saito, T.; Yoshida, Z. *Tetrahedron* **1972**, *28*, 3191–3201. (c) Mazur, Y.; Bock, H.; Lavie, D. *Can. Pat. Appl.* 2,029,993, 1991. (d) Clar, E. *J. Chem. Soc.* **1949**, 2013–2016.

(16) (a) Jiang, D.-E.; Sumpter, B. G.; Dai, S. *J. Chem. Phys.* **2007**, *127*, 124703. (b) Jiang, D.-E.; Dai, S. *Chem. Phys. Lett.* **2008**, *466*, 72–75.

(17) (a) Arabei, S. M.; Pavich, T. A. *J. Appl. Spectrosc.* **2000**, *67*, 236–244. (b) Kuroda, H. *J. Chem. Soc.* **1960**, 1856–1857. (c) Clar, E. *Chem. Ber.* **1948**, *81*, 52–63.

(18) Yao, J.; Chi, C.; Wu, J.; Loh, K. *Chem.—Eur. J.* **2009**, *15*, 9299–9302.

**Scheme 1.** Synthetic Route of Compounds **3** and **4**



first prepared according to the literature.<sup>17</sup> Reaction of **5** with the lithium reagent of (4-bromo-2,6-di-*tert*-butylphenoxy)-

rimethylsilane<sup>19</sup> generated by lithium–halogen exchange reaction gave the alcohol **6** in 74% yield. Subsequent desilylation of **6** with tetrabutylammonium fluoride (TBAF) and dehydration of the as-formed phenol by POCl<sub>3</sub> in pyridine afforded the desired bisanthracenequinone **4** in 56% yield for two steps. The product **4** precipitated from the solution as a light yellow powder, and simple purification by filtration and washing with ethanol is sufficient to give the pure compound. However the synthesis of compound **3** by photocyclization reaction of **4** in benzene failed due to the decomposition of starting materials. Alternatively, the compound **3** was prepared by a similar synthetic route starting from the bisanthenequinone **2**. We also found that reaction of **2** with the same lithium reagent gave a complicated mixture but reaction with the Grignard reagent of (4-bromo-2,6-di-*tert*-butylphenoxy)trimethylsilane worked well, and the target compound **7** was obtained in 66% yield. Subsequent desilylation and dehydration of **7** under similar conditions provided the final product **3** as a dark green solid in 20% yield. The chemical structures and purity of all new compounds were verified by <sup>1</sup>H NMR, <sup>13</sup>C NMR, elemental analysis, mass spectrometry (EI, HR-EI or MALDI-TOF), and FT-IR spectroscopy (see the Supporting Information). Both **3** and **4** exhibited sharp NMR signals in organic solvents even at elevated temperature (e.g., 100 °C in 1,2-dichlorobenzene-*d*<sub>4</sub>), indicating that both molecules exist in the form of quinone instead of biradicals. Their quinoidal structure was further confirmed by their FT-IR spectra (Figure S1, Supporting Information). The intense bands at 1650 cm<sup>-1</sup> for **3** and 1613 cm<sup>-1</sup> for **4** are assigned to the C=O stretching vibration. Both compounds also showed quite good thermal stability as determined by thermogravimetric analysis (TGA), and the initial thermal decomposition temperatures (*T*<sub>d</sub>) are 355 and 340 °C for **3** and **4**, respectively (Figure S2, Supporting Information).

Compounds **3** and **4** are soluble in chlorinated solvents such as dichloromethane (DCM), chloroform, and chlorobenzene, and the UV–vis–NIR absorption spectra of **3**–**5** are shown in Figure 2A. Solution of **3** in DCM displays a dark green color, and well-resolved absorption bands between 500 and 800 nm with the peak at 690 nm (log ε = 4.7; ε: molar extinction coefficient in M<sup>-1</sup> cm<sup>-1</sup>) are observed. Additional bands in the UV range are also found. The quinone **4**, however, mainly exhibits absorption from 300 to 500 nm with the peak at 428 nm (log ε = 5.2), and the solution of **4** in DCM shows a yellow color. There is a 34 nm red-shift compared with the absorption spectra of quinone **5**, indicating that π-conjugation is further extended in **4** by incorporating di-*tert*-butyl benzoquinone moieties. The significant red-shift (262 nm) in the absorption of **3** in comparison with **4** indicates largely enhanced π-conjugation in the rigid bisanthene-based quinone. In addition, although the bisanthenequinone **2** is insoluble in organic solvents, it can be dissolved in concentrated sulfuric acid, showing a low energy absorption peak at 572 nm (log ε = 4.2).<sup>17a</sup>

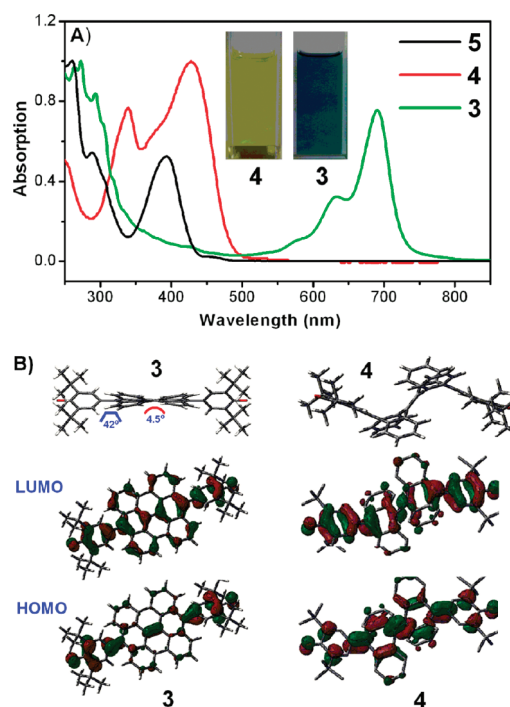


**Figure 2.** (A) UV–vis–NIR absorption spectra of compounds **3**–**5** in DCM ( $1.0 \times 10^{-5}$  M). (Inset) photos for dilute solutions of **3** and **4** in DCM. (B) Calculated molecular structures and frontier molecular orbital profiles for **3** and **4**.

For comparison, solution of **3** in concentrated sulfuric acid displays long-wavelength absorption bands with a maximum at 700 nm (log ε = 4.5, see Figure S3, Supporting Information). These data proved that the further extension of quinoidal structure in the bisanthenequinone resulted in extended conjugation along the long axis and led to NIR absorption. Furthermore, the molecule **3** can be also regarded as an analogue of the very unstable *p*-quarterphenoquinone,<sup>5c,f</sup> with the two center quinoidal benzene rings replaced by a quinoidal bisanthene unit. The solution of quinone **3** is very stable at ambient conditions and even upon exposure to 4 W UV lamp for several days. In comparison with a stable thiophene-containing heteroquarterphenoquinone<sup>5</sup> and the bisanthene itself, the absorption maximum of **3** exhibited 12 and 28 nm red-shifts, respectively. The molecular structures and the frontier molecular orbital profiles of **3** and **4** were calculated using DFT methods (Figure 2B; see the Supporting Information for details).

Molecule **3** has a distorted bisanthene unit with an out-of-plane distortion angle of approximately 4.5° relative to the central quinoidal benzene rings. The dihedral angle between the bisanthene unit and the terminal benzoquinone is about 42°, presumably due to steric congestion. Even with such a distorted structure, **3** exhibits efficient π-conjugation along the bisanthene and the benzoquinone units as can be

(19) Takahashi, K.; Suzuki, T.; Akiyama, K.; Ikegami, Y.; Fukazawa, Y. *J. Am. Chem. Soc.* **1991**, *113*, 4576–4583.

(20) Brédas, J. L.; Chance, R. R.; Baughman, R. H.; Silbey, R. *J. Chem. Phys.* **1982**, *76*, 3673–3678.

predicted by their electron cloud distribution in its LUMO and HOMO profiles.<sup>20</sup> In contrast, molecule **4** has a central-symmetric, double-saddle-like structure due to the strong steric congestion at the anthracene/anthracene and benzoquinone–anthracene interfaces. Nevertheless, electron delocalization can still be observed along the long axis, with the bond length alternation showing a typical quinoidal character. Such a difference in conformation and  $\pi$ -conjugation explains their big difference in electronic properties. In agreement with the absorption spectra, fluorescence spectra of **3** and **4** in DCM show emission peaks at 726 and 455 nm, respectively (Figure S4, Supporting Information).

Cyclic voltammetry was employed to investigate the redox behavior of **3** and **4**. As shown in Figure 3A, **3** in

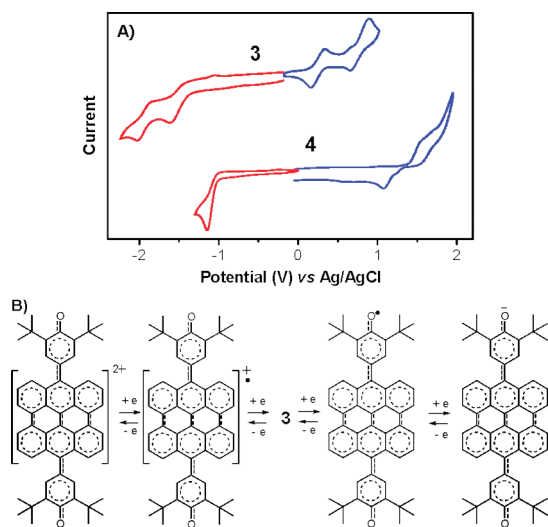


**Figure 3.** (A) Cyclic voltammograms of compounds **3** (in chlorobenzene) and **4** (in dichloromethane) with 0.1 M Bu<sub>4</sub>NPF<sub>6</sub> as supporting electrolyte, AgCl/Ag as reference electrode, gold disk as working electrode, and Pt wire as counter electrode. (B) Four stable redox states of **3** through the amphoteric redox processes.

chlorobenzene exhibits clear amphoteric multistage redox behavior, consisting of two reversible one-electron oxidation waves ( $E_{1/2}^{\text{ox}} = 0.22, 0.71$  V vs AgCl/Ag) and two reversible one-electron reduction waves ( $E_{1/2}^{\text{red}} = -1.42, -1.86$  V vs AgCl/Ag). The multistage reversible redox waves provide evidence for the formation of stabilized singly and doubly charged species of quinone **3**, i.e., the dication, radical cation, radical anion, and dianion (Figure 3B). The charged states of **3** were also studied by chemical oxidation and reduction titrations followed by absorption spectroscopic measurements (Figure S5, Supporting Information). Compound **3** was oxidized into stable radical cation by iodine and further to stable dication by stronger oxidant such as SbCl<sub>5</sub>. The oxidized species can be reversibly reduced into a neutral state by Zn dust. Meanwhile, **3** can also be reduced by lithium

directly into a dianion state. Thus, compound **3** is characterized as a new quinone material exhibiting a high amphoteric redox behavior with a small span ( $E^{\text{sum}} = E_{1/2}^{\text{ox}} + (-E_{1/2}^{\text{red}}) = 1.64$  V) of the oxidation and reduction potentials. In contrast, compound **4** in DCM shows one irreversible reduction wave and one quasi-reversible oxidation wave.

The large peak–peak separation ( $\Delta E_p = 450$  mV) in the oxidative wave of **4** indicates possible large conformation change during the transition between the neutral and radical cation, a phenomenon usually observed in highly distorted  $\pi$ -systems.<sup>7b,21</sup> Compared with **4**, the first reduction peak of **3** is shifted to a more negative value by 0.4 V due to low electron affinity of the bisanthene core. The large  $\pi$ -conjugated system in **3** also stabilizes the charged species created during the amphoteric redox processes. The very different redox behavior between **3** and **4** indicates the importance of rigid planar structure on the electrochemical amphoterism. The HOMO and LUMO energy levels of **3** and **4** were also determined from the onset potentials of the oxidation and reduction waves,<sup>22</sup> and it turns out that compound **3** has a higher lying HOMO ( $-4.52$  eV for **3** vs  $-5.74$  eV for **4**) and LUMO energy levels ( $-2.95$  eV for **3** vs  $-3.32$  eV for **4**) due to the electron donating character of the bisanthene unit. The compound **3** also has a smaller band gap (1.57 eV) than **4** (2.42 eV), and as a result, long wavelength absorption was observed.

In summary, we have successfully synthesized a soluble and stable bisanthenequinone which shows intense NIR absorption and amphoteric redox behavior. Compound **3** represents a rare example of quinoidal large polycyclic aromatic hydrocarbons which are supposed to show interesting opto-electronic properties. The observed material properties for **3** such as intense NIR absorption, electrochemical amphoterism and good thermal and photostability qualify it as a useful NIR dye for many potential applications such as NIR laser filter, optical data recording and ambipolar charge transporting materials. The synthetic strategy reported in this work also provides clues to develop higher order soluble and stable quinoidal polycyclic hydrocarbons such as periacenes in the future.

**Acknowledgment.** This work was financially supported by a NRF Competitive Research Program (R-143-000-360-281) and a NUS Young Investigator Award (R-143-000-356-101).

**Supporting Information Available:** Experimental details and characterization data of all new compounds and details for DFT calculations. This material is available free of charge via the Internet at <http://pubs.acs.org>.

OL902241U

(21) Bryce, M. R.; Coffin, M. A.; Hursthouse, M. B.; Karaulov, A. I.; Müllen, K.; Scheich, H. *Tetrahedron Lett.* **1991**, *32*, 6029–6032.

(22) Pommerehne, J.; Vestweber, H.; Guss, W.; Mahrt, R. F.; Baessler, H.; Porsch, M.; Daub, J. *Adv. Mater.* **1995**, *7*, 551–554.